Fruit Research

ARTICLE

Open Access

https://doi.org/10.48130/frures-0026-0034

Fruit Research **2026**, 6: e040

Metabolite profiling of peel and flesh across harvest stages in Pawpaw (*Asimina triloba*) fruit

Griffin John Erich[1], Zhangjun Fei[2] and Yosef Al Shoffe[1*]

[1] *Horticulture Section, School of Integrative Plant Science, College of Agriculture and Life Science, Cornell University, Ithaca, NY 14853, USA*
[2] *Boyce Thompson Institute, Ithaca, NY 14853, USA*
* Correspondence: yas24@cornell.edu (Al Shoffe Y)

Abstract

Pawpaw (*Asimina triloba*; family Annonaceae) is the largest edible fruit native to the eastern United States. Fruit typically develop in clusters of one to six per flower and ripen between mid-August and mid-October, depending on genotype and growing location. In this study, 'Shenandoah™' pawpaw fruits were harvested from Deep Run Pawpaw Orchard (Westminster, MD) at three harvest times–early, optimum, and late–at weekly intervals. Fruit maturity was assessed at harvest, and metabolic profiles were analyzed separately for peel and flesh tissues. Flesh firmness, dry matter content, Index of absorbance difference (I_{AD}) value, and L^* and b^* color parameters decreased with advancing harvest time, whereas a^* values increased. Flesh firmness, dry matter content, and L^* values were higher on the shaded side of the fruit compared with the sun-exposed side, while a^* values were higher on the sun-exposed side. Primary and secondary metabolite levels, averaged by compound class, were affected by harvest time, and a slight increase in flavonoids was observed at the third harvest compared with the earlier harvests. Across all harvests, alkaloids, flavonoids, phenolics, quinones, and tannins were more abundant in the peel, whereas amino acids and their derivatives, as well as lipids, were present at lower levels in the peel than in the flesh. Nevertheless, the metabolite profile of both peel and flesh varied with harvest time, and tissue-specific changes were evident. Ethylene-related metabolites were consistently present across tissues and stages, but coordinated shifts in hormone crosstalk after H2 indicate a transition toward ripening-associated signaling. Pawpaw flesh accumulates high sugars early that decline, while the peel maintains more stable, protective sugars across harvests. Pawpaw peel is enriched in structural hydroxy fatty acids and saturated lipids, whereas the flesh contains a more diverse set of oxidized fatty acids and sphingolipid intermediates. Overall, this study demonstrates distinct metabolic differences between peel and flesh across different harvest times and highlights their influence on fruit quality, consumer acceptability, and potential pharmaceutical compounds.

Keywords: Pawpaw (*Asimina triloba*), Fruit maturity, Fruit quality, Widely targeted metabolomics

Citation: Erich GJ, Fei Z, Al Shoffe Y. 2026. Metabolite profiling of peel and flesh across harvest stages in Pawpaw (*Asimina triloba*) fruit. *Fruit Research* 6: e040 https://doi.org/10.48130/frures-0026-0034

Introduction

Pawpaw is the largest native edible tree fruit in the United States[1–3]. The tree naturally occurs in the forest understory in large clonal patches as well as along riparian edges. When planted in full sun, pawpaw trees can reach heights surpassing 10 meters and produce more fruit relative to shaded conditions.

Pawpaw fruit is large and oblong-cylindrical in shape, with lengths ranging from 3 to 15 cm and widths from 3 to 10 cm[4,5]. Brannan et al.[5] reported variation in fruit mass among pawpaw cultivars, ranging from 122 to 292 g, with an average mass of 194 g. The taste of pawpaw fruit has been described as a blend of mango, banana, and pineapple, while maintaining a custard-like texture[1,6]. Several studies have investigated the metabolic profile of pawpaw fruit. For example, Nam et al.[7] reported that the most abundant carbohydrates in pawpaw fruit are sucrose, followed by glucose and fructose. The dominant organic acid in pawpaw fruit is acetic acid, followed by formic, oxalic, malic, and citric acids[7]. Total soluble solids and titratable acidity have been shown to vary significantly among cultivars[8]. Importantly, the metabolite profile of pawpaw fruit has been shown to change throughout the storage period. The cultivar 'Tollgate' exhibits high carotenoid levels during the first 21 days of storage, whereas 'KSU Atwood' tends to accumulate higher levels of carotenoids in overripe fruit[9]. Total carotenoid content showed a moderate positive correlation with b^* and chroma values in pawpaw pulp[9]. Gas chromatography-olfactometry (GC-O) has also been used to identify odor compounds in pawpaw fruit, including acetaldehyde, diacetyl, eugenol, homofuraneol, delta-octalactone, gamma-octalactone, and vanillin. In addition, 3-hydroxyethyl butyrate was identified as a marker compound to distinguish the cultivar 'Mango' from other cultivars[10].

Annonaceous acetogenins have been identified in pawpaw fruit[11,12]. These compounds have also been found in the flesh of both unripe and ripe fruit, with concentrations decreasing throughout the growing season[7,12,13]. These compounds are also present in the leaves, bark, and seeds[11]. It has been hypothesized that the pawpaw peel contains a higher level of acetogenins than the flesh, which may contribute to the inedible nature of the pawpaw peel.

Metabolomics is a powerful technique that enables the comprehensive detection of plant metabolites. Widely targeted metabolomics provides important information on relative differences among many known metabolites between the flesh and peel of pawpaw fruit and a better understanding of the composition of both parts of the fruit. Given the numerous health benefits associated with pawpaw, there is emerging commercial potential for this fruit crop. Understanding the metabolite profile across harvests can provide insight into the nutritional value of pawpaw fruit at different stages of maturity. In addition, identifying differences in metabolite composition between peel and flesh may reveal compounds contributing to the unpleasant taste of the fruit's exterior. Our study focuses on the widely targeted metabolome of peel and flesh tissues of the cultivar 'Shenandoah™' across three harvest dates in relation to fruit maturity.

© The Author(s)

https://doi.org/10.48130/frures-0026-0034

Materials and methods

Fruit of the pawpaw cultivar 'Shenandoah™' were collected at different maturity stages from the Deep Run Pawpaw Orchard in Westminster, MD. A total of 450 fruit—150 at each harvest date—were harvested at three time points: 1 week before the anticipated commercial harvest date (H1), at the anticipated harvest date (H2), and 1 week after commercial harvest (H3). At each harvest, fruit weight, dry matter content, firmness, and skin color were measured using a Chroma Meter (CR-400, Japan). Skin color parameters included L^* (lightness; 0 = black to 100 = white), a^* (– = green to + = red), b^* (– = blue to + = yellow), and I_{AD} (index of absorbance difference). All color measurements were recorded on both the sun-exposed and shaded sides of the fruit. Peel tissue strips from both sides and flesh tissue were collected from 10 fruit per replicate, frozen in liquid nitrogen, and stored at –80 °C for subsequent analyses. Flesh firmness was measured using an automatic pressure tester (Guss Manufacturing (Pty) Ltd, Strand, South Africa) equipped with a 1-mm-diameter probe. All maturity assessments were conducted at the Cornell Postharvest Laboratory using the methods described by Al Shoffe et al.[14].

UPLC–MS/MS analysis

Samples were lyophilized using a vacuum freeze-dryer and ground in a ball mill grinder (MM 400, Retsch) at 30 Hz for 1.5 min. For extraction, 50 mg of ground material was mixed with 1,200 μL of pre-chilled (–20 °C) 70% methanol containing internal standards. The mixture was vortexed for 30 s every 30 min for six cycles, followed by centrifugation at 12,000 r/m for 3 min at 4 °C. The supernatant was filtered through a 0.22-μm membrane and used for UPLC–MS/MS analysis (ExionLC™ AD UPLC system, AB Sciex LLC, Framingham, MA, USA).

Untargeted metabolomic profiling was first performed for metabolite identification. Qualitative identification of metabolites was conducted using the MWDB (Metaware database) based on accurate mass, MS^2 fragmentation patterns, isotopic distribution, and retention time. Secondary spectral information was used to further confirm metabolite identity. Isotopic peaks, redundant ion signals (K^+, Na^+, NH_4^+), and fragment-derived duplicates were removed during data processing.

Quantification was performed using triple quadrupole mass spectrometry in multiple reaction monitoring (MRM) mode. In this mode, the first quadrupole selects precursor ions of target compounds, which are fragmented in the collision chamber. The third quadrupole then isolates characteristic product ions, minimizing interference and enabling accurate and reproducible quantification[15].

Data preprocessing

Raw data were processed by first imputing missing values with one-fifth of the minimum value for each metabolite. Coefficients of variation (CVs) from quality control samples were then calculated, and metabolites with a CV < 0.5 were retained, resulting in the final dataset[16].

Statistical analysis

Statistical analyses included coefficient of variation (CV), principal component analysis (PCA) using R (base package) v4.1.2, ring plots, Pearson's correlation using R (base package) v4.1.2, hierarchical cluster analysis (HCA), volcano plots, chord diagrams using R (igraph; ggraph) v1.2.11; 2.0.5, Venn diagrams, K-means clustering (was applied as an unsupervised pattern-recognition method to group metabolites based on similarities in their abundance profiles across samples. The resulting clusters reflect shared accumulation trends, not chemical structure; therefore, each cluster may contain metabolites from multiple chemical classes that exhibit similar quantitative patterns) using R (base package) v4.1.2, and Kyoto Encyclopedia of Genes and Genomes (KEGG) pathway analysis[17,18]. Mean differences were evaluated using Tukey's HSD test, Student's t-test, and least significant difference (LSD) at the 5% significance level. Data visualization and statistical analyses were performed using JMP software (JMP 19 Student Edition).

Results

Flesh firmness and dry matter content were significantly influenced by both harvest timing and canopy position. As harvest progressed, a significant reduction in firmness (3.4 to 1.1 N) was observed, accompanied by a decrease in L^* and an increase in a^*, reflecting the transition from green to darker, more mature skin coloration. Regarding solar exposure, shaded fruit maintained higher firmness and dry matter content compared with sun-exposed fruit, although the index remained consistent between the two sides (Table 1).

A total of 2,266 metabolites were detected in pawpaw fruit. The major metabolite classes included alkaloids (14.4%), amino acids and derivatives (10.4%), flavonoids (17.4%), lignans and coumarins (5.0%), lipids (9.0%), nucleotides and derivatives (3.2%), organic acids (3.8%), phenolics (11.1%), quinones (0.8%), steroids (0.1%), tannins (1.2%), terpenoids (8.3%), and other compounds (15.2%) (Fig. 1a). Coefficient of variation (CV) analysis indicated that more than 85% of detected peaks in both peel and flesh samples were stable and reproducible (Fig. 1b). Hierarchical clustering analysis (HCA) revealed clear metabolic distinctions between peel and flesh tissues based on Z-score–standardized metabolite profiles (Fig. 1c).

Table 1. Fruit maturity of 'Shenandoah™' at harvest, including measurements of flesh firmness, dry matter content, I_{AD} value, L^*, a^*, and b^* from sunny and shaded sides for fruit harvested in three harvests at weekly intervals in 2024.

		Flesh firmness (N)	Dry matter content (%)	I_{AD} value	L^*	a^*	b^*
Harvest	1	3.4 a	25.9 a	2.24 a	60.7 a	–13.2 c	35.3 a
	2	1.8 b	24.7 b	2.19 a	60.0 a	–11.8 b	35.1 a
	3	1.1 c	24.0 b	1.88 b	54.2 b	–7.3 a	31.5 b
	***p*-value**	**< 0.0001**	**0.0002**	**< 0.0001**	**< 0.0001**	**< 0.0001**	**< 0.0001**
Fruit side	Sunny	1.8 b	22.4 b	2.09	57.4 b	–7.6 a	34.2
	Shaded	2.4 a	27.4 a	2.11	59.2 a	–13.9 b	33.7
	***p*-value**	**0.0023**	**< 0.0001**	**0.3963**	**0.004**	**< 0.0001**	**0.4086**

Different letters in the same column indicate significant differences at p value < 0.05 (in bold).

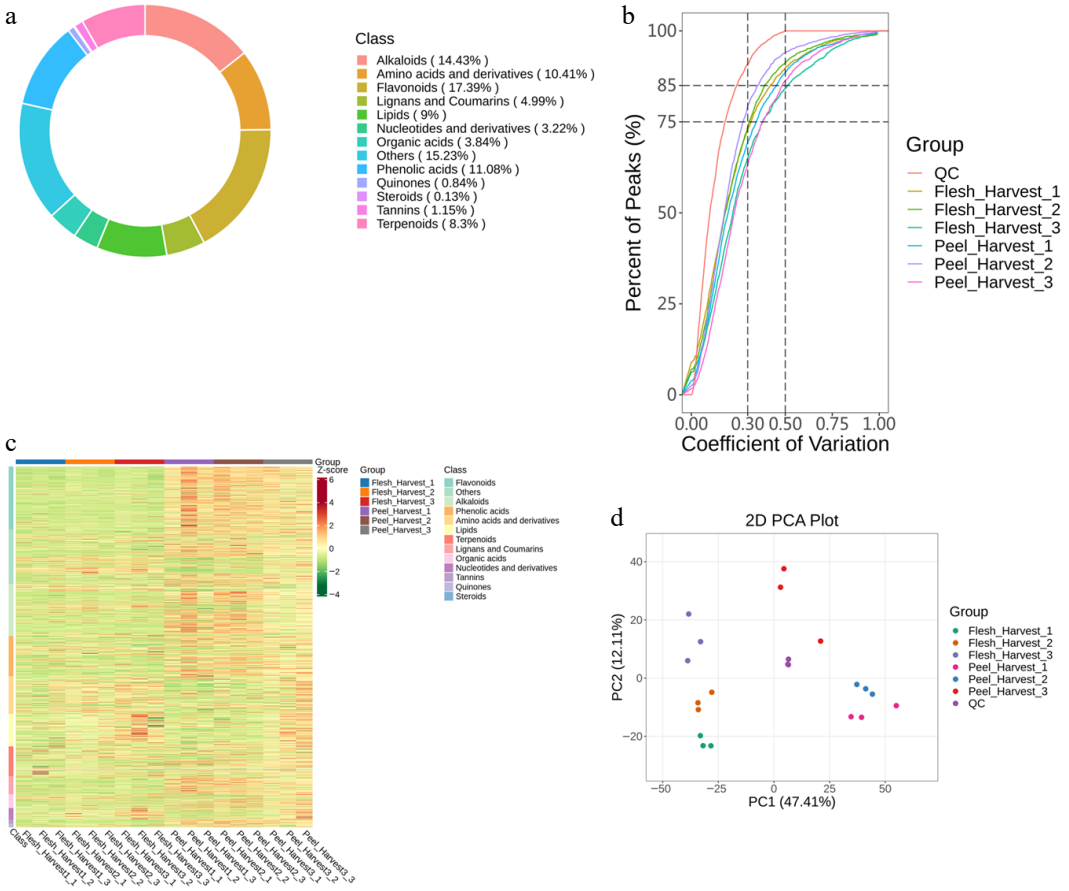


Fig. 1 (a) Ring plot of metabolite categories. (b) CV distribution of each group. (c) Hierarchical Cluster Analysis (HCA). (d) PCA score diagram of quality spectrum data of each group of samples and quality control samples.

Principal component analysis (PCA) further separated peel and flesh samples, with PC1 and PC2 together explaining 60% of the total variance (Fig. 1d).

Volcano plot analysis revealed 1,412, 1,468, and 1,616 metabolites in peel and flesh tissues of fruit at H1, H2, and H3, respectively. Among these, 609, 595, and 550 compounds were upregulated; 220, 192, and 81 were downregulated; and 583, 681, and 985 showed no significant differences in peel compared with flesh at H1, H2, and H3, respectively (Fig. 2a–c). Across harvests, 2,054 metabolites were detected in flesh tissues. Compared with H1, flesh at H2 contained 91 upregulated and 19 downregulated compounds (Fig. 2d). Flesh at H3 showed 194 upregulated, 40 downregulated, and 1,714 nonsignificant compounds relative to H1 (Fig. 2e). A total of 2,082 metabolites were shared between H2 and H3 flesh samples, among which 71 were upregulated and 35 were downregulated at H3 compared with H2 (Fig. 2f). Peel tissues also exhibited substantial metabolic variation across harvests. Among the 2,121 metabolites detected in peels at H1 and H2, 100 were upregulated, and 12 were downregulated in H2 compared with H1 (Fig. 2g). Compared with H3, peels at H1 contained 97 higher and 232 lower metabolites (Fig. 2h). Peels at H3 showed 130 upregulated and 183 downregulated compounds compared with H2 (Fig. 2i).

Correlation network analysis revealed a highly integrated metabolic landscape characterized by dense clusters of positive correlations across diverse chemical classes, including flavonoids, amino acids, and terpenoids in peel and flesh at H1 (Fig. 3a), flavonoids, amino acids, and lipids at H2 (Fig. 3b), and flavonoids, terpenoids, and phenolic acids at H3 (Fig. 3c). The differential accumulation of metabolites, evidenced by varying node sizes, indicates significant metabolic divergence between tissues, where protective secondary metabolites like phenolic acids and tannins (Fig. 3a, b) and tannins and alkaloids (Fig. 3c) showed coordinated co-expression patterns. The predominance of positive correlations suggests that the metabolic flux is governed by shared regulatory mechanisms, likely reflecting synchronized physiological responses to tissue-specific requirements such as defense in the peel vs. nutrient storage in the flesh.

Comparative analysis of differentially accumulated metabolites (DAMs) across the three harvest stages revealed dynamic metabolic transitions during fruit maturation. A total of 56 core metabolites were consistently identified as DAMs across all comparisons (H2 vs. H1, Flesh H3 vs. H1, and Flesh H3 vs. H2) (Fig. 3d), suggesting a stable metabolic signature throughout the ripening process. The highest degree of metabolic shift was observed between the first and third harvests, which yielded 144 unique DAMs. In addition, the transition between the second and third harvests revealed 158 shared DAMs not observed in the comparison between H2 vs. H1. These results indicate that while a subset of the metabolome undergoes early and sustained modification, the most substantial chemical divergence occurs during the later stages of maturity. In peel tissues, analysis of DAMs reveals a more complex metabolic shift than in flesh tissue (Fig. 3e). A core set of 62 metabolites was consistently identified as DAMs across all comparisons in peel (H2 vs. H1, H3 vs. H1, and H3 vs. H2), indicating a foundational set of compounds undergoing continuous modification during peel maturation. Notably, the transition between H2 and H3 exhibited the most substantial divergence, with 307 shared DAMs, nearly double the

https://doi.org/10.48130/frures-0026-0034

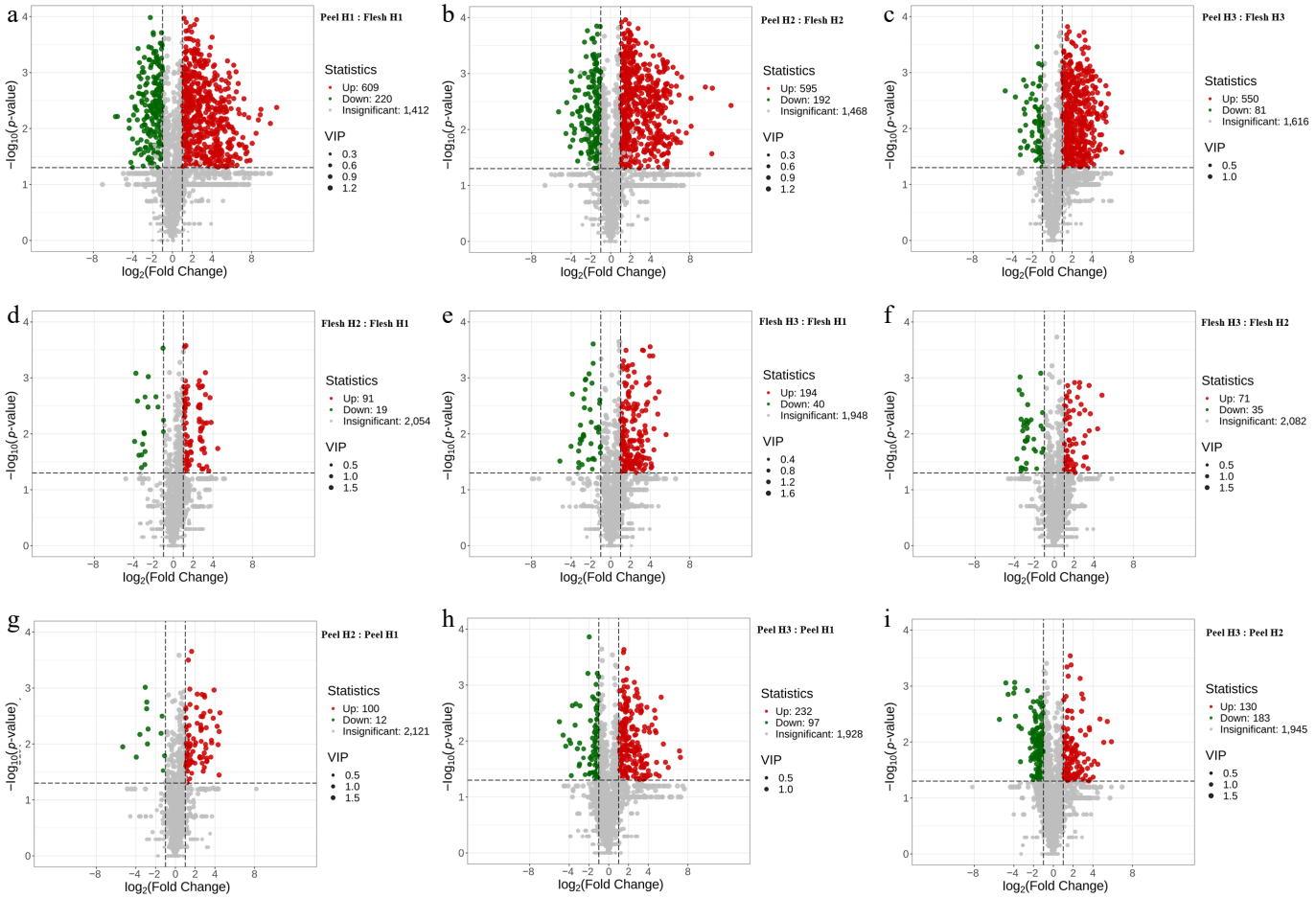


Fig. 2 Volcano plot of differential metabolites for (a) peel H1 : flesh H1, (b) peel H2 : flesh H2, (c) peel H3 : flesh H3, (d) flesh H2 : flesh H1, (e) flesh H3 : flesh H1, (f) flesh H3 : flesh H2, (g) peel H2 : peel H1, (h) peel H3 : peel H1, and (i) peel H3 : peel H2. Each point in the volcano plot represents a metabolite, with green dots representing downregulated differential metabolites, red dots representing upregulated differential metabolites, and gray dots representing the detected metabolites but showing no significant differences. The X-axis represents the Log_2FC value of metabolites between two groups. The further away from 0 on the X-axis, the greater the fold-change between two groups. If the metabolites were screened using VIP + FC + *p*-value, the Y-axis will represent the level of significant differences ($-Log_{10}$ *p*-value). The size of each dot represents the VIP value. If the metabolites were screened using VIP + FC, the Y-axis will represent the VIP value. The larger the VIP value, the more significant the difference and the more reliable the screening process.

158 shared DAMs observed in flesh during the same interval. Additionally, the peel exhibited 127 unique DAMs between H1 and H3, further underscoring specialized accumulation of secondary metabolites associated with environmental adaptation and fruit protection. Collectively, these results suggest that while both tissues undergo significant ripening-related changes, peel tissues maintain a significantly higher degree of metabolic turnover and unique chemical flux during the final stages of fruit development. The Venn diagram (Fig. 3f) further revealed substantial metabolic differences between peel and flesh tissues, with 728 DAMs shared across all three harvest stages.

K-means clustering revealed clear developmental differences in pawpaw fruit across harvest dates, identifying four subclasses each for flesh and peel tissues (Fig. 4), with standardized trait trajectories showing that fruit did not follow a uniform ripening pattern but instead separated into multiple biologically meaningful groups. In the flesh, subclasses were uneven in size (810, 177, 314, and 366 samples) and displayed highly divergent temporal patterns: one large group showed only modest change across harvests, another exhibited a strong increase from Harvest 1 to 3, a third showed a decreasing trend suggestive of delayed ripening, and a fourth displayed moderate but consistent increases. These patterns indicate substantial physiological heterogeneity within the flesh, even among fruit harvested at the same stage. Peel tissue also separated into four subclasses (623, 652, 257, and 190 samples), but with more uniform cluster sizes and generally more moderate trajectories: one group remained stable across harvests, another increased gradually, a third decreased slightly, and a small fourth group showed a sharp late-stage rise. Compared with flesh, peel exhibited less within-cluster variability and smaller amplitude changes, suggesting more conserved or uniform responses to ripening. Together, these results show that flesh and peel tissues follow distinct maturation pathways, with flesh displaying greater heterogeneity and peel showing more consistent developmental behavior, highlighting asynchronous ripening dynamics and substantial biological variation within harvest dates. KEGG (Kyoto Encyclopedia of Genes and Genomes) pathway analysis of the comparison H2 vs. H1 in flesh revealed that differentially accumulated metabolites were predominantly associated with the metabolism category, which accounted for the majority of the observed shifts. Within this category, metabolic pathways (63.27%) and biosynthesis of secondary metabolites (38.78%) were the most highly represented, followed by significant enrichment for purine metabolism, nucleotide metabolism, and flavone and flavonol biosynthesis (each 10.2%). Smaller percentages of metabolites

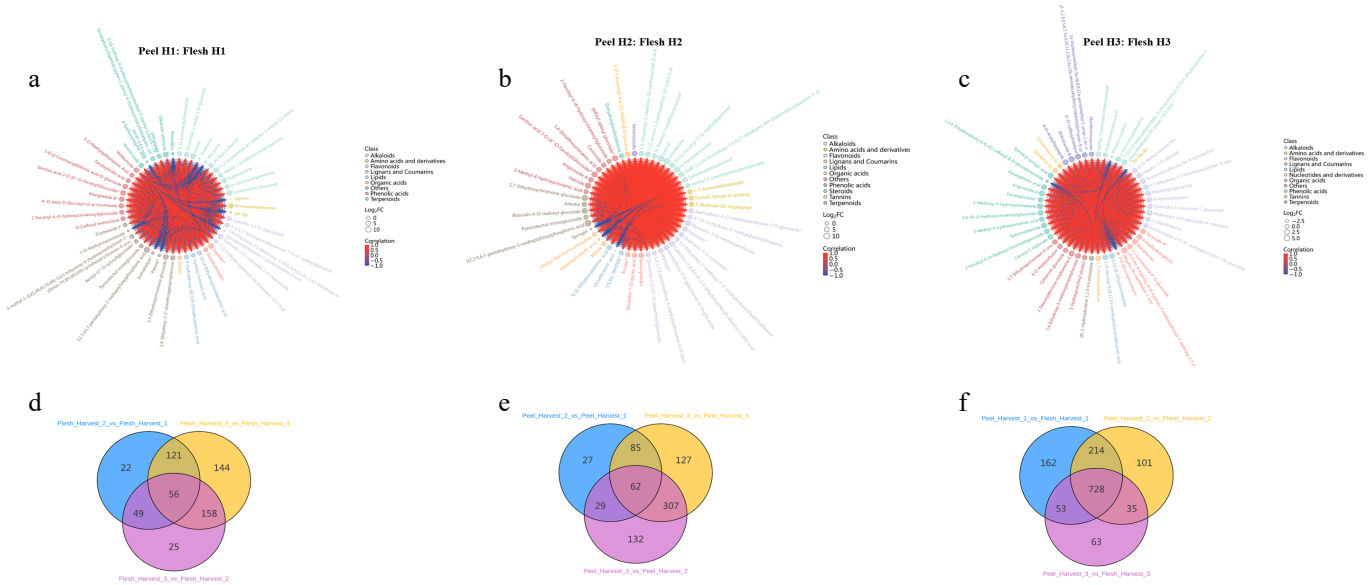


Fig. 3 Chord diagram of differential metabolites for (a) peel H1 : flesh H1, (b) peel H2 : flesh H2, and (c) peel H3 : flesh H3. The outermost layer shows the metabolite ID, and the second layer shows the Log_2FC value; the larger the dot, the larger the Log_2FC value. The color for the first and second layers represents Class I metabolite classification. The chords in the innermost layer reflect the Pearson correlation between the connected metabolites. Red chords represent positive correlation, and blue chords represent negative correlation. If there are more than 50 differential metabolites, the figure will only show the top 50 metabolites based on VIP. (d)–(f) represent Venn diagrams of differences among groups for peel and flesh. Each circle represents a comparison group; the number in overlapped parts represents the number of common differential metabolites between comparison groups, and the number in non-overlapped parts represents the number of unique differential metabolites in comparison groups.

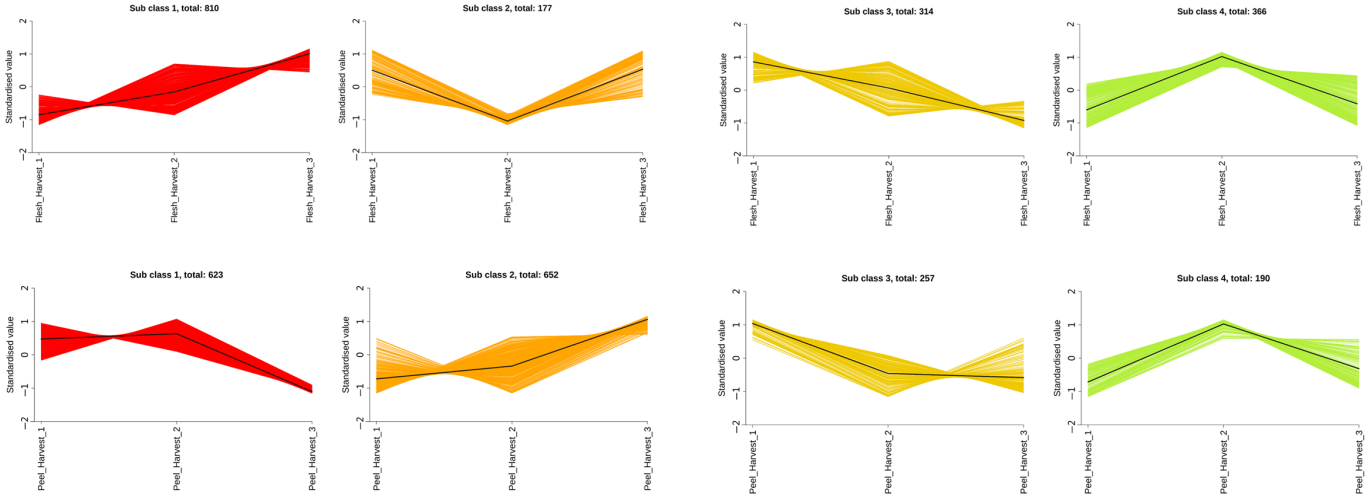


Fig. 4 K-means diagram of differential metabolites. The X-axis represents the sample names, and the Y-axis represents the normalized relative quantification. 'Sub class' represents a group of metabolites with the same trend, and 'total' represents the number of metabolites in this cluster.

were also associated with environmental information processing via plant hormone signal transduction and ABC transporters, indicating that the transition between early harvest stages in flesh tissues involves substantial reconfiguration of primary energy pathways and the specialized synthesis of antioxidant compounds (Supplementary Fig. S1).

For the H3 vs. H1 comparison in flesh tissues, metabolic activity intensified as the fruit reached full maturity. While the primary changes remained within the Metabolism category, the proportion of metabolites associated with metabolic pathways increased to 67.37%, and biosynthesis of secondary metabolites rose to 45.26%, indicating a broader chemical shift than that observed in the earlier transition from H1 to H2. Notably, enrichment in biosynthesis of cofactors (15.79%), purine metabolism (11.58%), and Linoleic acid metabolism (11.58%) suggests that late-harvest flesh development is characterized by the accumulation of fatty acids and specialized compounds, further supported by continued ABC transporter activity (10.53%), which may facilitate nutrient sequestration (Supplementary Fig. S2).

KEGG classification of the H3 vs. H2 comparison in flesh tissues highlighted continued core metabolic restructuring during the final stages of fruit maturity. Although metabolic pathways remained the dominant category (69.81%), notable enrichment was observed in biosynthesis of cofactors (18.87%) and biosynthesis of secondary metabolites (39.62%), indicating a shift toward specialized compound accumulation rather than broad pathway reorganization. Enrichment in isoflavonoid biosynthesis (9.43%) and ascorbate and aldarate metabolism (9.43%) further suggests that late-harvest flesh

https://doi.org/10.48130/frures-0026-0034

development involves fine-tuning of antioxidant metabolism and specific flavor-related precursors, supported by continued activity of ABC transporters (5.66%) associated with environmental information processing (Supplementary Fig. S3).

KEGG classification of the comparison between peel and flesh at H1 highlighted fundamental metabolic distinctions between the two tissues at the early harvest stage. The metabolism category dominated the profile, with metabolic pathways involving 66.82% of the differentially accumulated metabolites and biosynthesis of secondary metabolites accounting for 45.33%. Specifically, peel tissues showed high enrichment in defensive and structural pathways compared to flesh tissues, including Isoquinoline alkaloid biosynthesis (7.94%), flavonoid biosynthesis (8.88%), and flavone and flavonol biosynthesis (7.48%), alongside a significant reliance on ABC transporters (11.21%) for metabolite translocation (Supplementary Fig. S4).

KEGG classification of the peel vs. flesh comparison at H2 underscored substantial divergence in secondary metabolism and protective signaling between the two tissues at the mid-developmental stage. Within the dominant Metabolism category, metabolic pathways and biosynthesis of secondary metabolites remained the primary drivers of differentiation, accounting for 63.83% and 44.68% of the differentially accumulated metabolites, respectively. At this stage, peel tissues showed higher enrichment in antioxidant and defensive pathways compared with flesh tissues, including flavonoid biosynthesis (10.11%), isoquinoline alkaloid biosynthesis (7.98%), and flavone and flavonol biosynthesis (8.51%). Peel tissues also maintained substantial activity of ABC transporters (10.64%) (Supplementary Fig. S5).

KEGG classification of the peel vs. flesh comparison at H3 identified the most pronounced metabolic divergence between the two tissues. While metabolism remained the dominant functional category, metabolic pathways and biosynthesis of secondary metabolites accounted for 60.45% and 49.25% of the differentially accumulated metabolites, respectively. At this late harvest stage, peel tissues were highly enriched in antioxidant- and pigment-related pathways compared with flesh tissues, including flavonoid biosynthesis (12.69%), isoquinoline alkaloid biosynthesis (11.19%), and flavone and flavonol biosynthesis (11.19%). This chemical specialization was further supported by continued activity of ABC transporters (8.21%) and increased representation of biosynthesis of cofactors (11.19%), illustrating a mature physiological state where the peel serves as a complex chemical shield for the nutrient-dense flesh (Supplementary Fig. S6).

Ethylene-related metabolism in fruit was active across both tissue types and all harvests, but its interaction with other hormone pathways shifts as ripening progresses (Supplementary Table S1). In both the flesh and peel, the core ethylene precursors, S-adenosyl-L-methionine, S-adenosyl-L-homocysteine, and methionine, were consistently present from H1 to H3. However, compounds associated with ethylene–jasmonate signaling (jasmonic acid and jasmonoyl-isoleucine) and JA-related derivatives appeared mainly at H2–H3. The presence of the JA precursor 12-oxo-phytodienoic acid only at H2 in both tissues points to a transient activation of upstream JA biosynthesis. Additionally, ABA-related crosstalk (abscisate) emerges at H2–H3, aligning with the hormonal coordination typical of climacteric ripening. Auxin-linked metabolites (tryptophan and indole derivatives) remain detectable from H1–H3 in the flesh (Supplementary Table S1).

Across the three harvests (H1–H3), sugars in pawpaw fruit showed distinct patterns between flesh and peel. In the flesh, monosaccharides (glucose and fructose) were very high at early harvest and decreased over time, while sucrose was very high, particularly in H1. Oligosaccharides remained at moderate levels in the flesh, whereas sugar phosphates were consistently present, reflecting ongoing metabolic activity. Polyols were also present at moderate concentrations. In contrast, the peel generally had moderate levels of monosaccharides and sucrose, but higher concentrations of oligosaccharides and moderate to high levels of polyols (Supplementary Table S2).

The fatty acid profile showed clear tissue-specific differences between pawpaw peel and flesh. The peel was enriched in structural and protective lipids, particularly hydroxy fatty acids (e.g., 12-hydroxyoctadecanoic acid and 9,16-dihydroxypalmitic acid) and saturated long-chain fatty acids like hexadecanoic acid. It also contained higher levels of certain oxylipins such as 13(S)-HOT and sphingoid compounds like hexadecylsphingosine. In contrast, the flesh exhibited a greater diversity and abundance of oxylipins, including TriHOMEs, HODEs, and HOT derivatives, indicating more active lipid oxidation processes. The flesh was also richer in highly oxygenated fatty acids and sphingolipid intermediates such as sphinganine and phytosphingosine (Supplementary Table S3).

Discussion

Across three harvest dates (H1–H3), 'Shenandoah™' pawpaw displayed clear and progressive ripening trends at harvest, including fruit softening, declining dry matter content, reductions in L^* and b^*, and increasing a^*. Canopy side effects were also observed, with shaded fruit generally firmer and exhibiting higher dry matter content and L^* values. In parallel, widely targeted metabolomics detected 2,266 metabolites and revealed strong tissue specificity: peel tissues consistently accumulated higher levels of defense-related secondary metabolite classes (e.g., alkaloids, flavonoids, phenolics, quinones, and tannins), whereas flesh tissues were relatively enriched in metabolites associated with primary metabolism, including amino acids and derivatives, as well as lipids. Together, multivariate analyses (HCA/PCA), volcano plot comparisons, correlation network analysis, K-means clustering, and KEGG pathway classification consistently indicate divergent physiological roles of peel and flesh tissues, with these metabolic differences becoming more pronounced as fruit maturity progresses.

The persistent enrichment of secondary metabolite classes in the peel across all harvest stages is consistent with the peel's role as the fruit's first line of defense. In peel tissues, phenylpropanoids, flavonoids, and related compounds contribute to UV screening, oxidative buffering, pigmentation, and anti-herbivory or antimicrobial functions. Similar peel-greater-than-flesh metabolite patterns have been widely reported in other fruit, including apple, pear, and kiwi berry[19–21]. In pawpaw, the prominence of alkaloids and related specialized metabolites in the peel is consistent with previous reports of *Annonaceous acetogenins* in fruit tissues and other plant organs[11,12,22]. These compounds may contribute to fruit quality characteristics, such as the non-edibility and bitterness of the peel, while also highlighting potential bioactivity and safety considerations for pawpaw-derived by-products.

Across the three harvests, the number and identities of DAMs indicate increasing metabolic divergence from early to late stages, with the largest shift occurring between H2 and H3, particularly in peel tissues. The chord network analyses revealed predominantly positive correlations among DAMs, suggesting shared regulatory controls. K-means clustering further identified large peel-dominant subclasses that remained elevated across harvest stages, alongside

flesh-dominant clusters consistent with metabolite accumulation related to storage and organoleptic development. KEGG classification consistently highlighted metabolic pathways and biosynthesis of secondary metabolites across all pairwise comparisons, with late-stage increases in cofactor biosynthesis and flavonoid-, flavonol-, and isoflavonoid-related pathways. Recurring enrichment of ABC transporters further suggests active metabolite translocation and sequestration during ripening. These patterns align with the broader coupling between optical ripening signals and biochemical change reported in nondestructive chlorophyll I_{AD} studies in other fruit[23–25].

Shaded fruit exhibited higher firmness, dry matter content, and *L** values than sun-exposed fruit at harvest. Such microclimate effects mirror horticultural evidence from apples showing that canopy position can modify optical and maturity indices, including I_{AD} and firmness, often with cultivar- and year-dependent variation[24,25].

Our dataset extends pawpaw research by: (1) separating peel and flesh metabolomes across multiple harvests for a named cultivar, provide direct evidence of tissue specialization that has been inferred from targeted observations[11,12,22]; (2) linking metabolite class behavior to objective maturity indices (firmness and color), providing a more integrated view than single-timepoint compositional reports[5,26]; and (3) framing ripening as a coordinated network phenomenon, characterized by predominantly positive correlations and ABC-transporter enrichment, an interpretation consistent with peel-greater-than-flesh antioxidant patterns observed in other species[19,20].

Priorities for future research include absolute quantification of sentinel compounds, such as flavonoids, phenolic acids, and selected alkaloids/acetogenins, in peel and flesh across maturity stages; integration with sensory and volatile profiles to assess consumer acceptance; multi-season and multi-cultivar replication to capture genotype x environment interactions; and safety-focused studies on peel and by-product processing streams. Field-deployable harvest tools that pair I_{AD} (or hyperspectral proxies) with metabolomics merit exploration[23,24]. Flesh-dominant metabolite clusters highlight biochemical features likely related to texture, sweetness, and flavor precursors; coupling these metabolomic signatures with sensory and consumer data could accelerate selection for eating quality, analogous to how peel-to-flesh phenolic ratios inform breeding in other fruit crops[19,21]. In terms of harvest timing, the largest metabolomic shift occurs between H2 and H3 in peel tissues, suggesting that even small delays beyond the 'optimum' window may disproportionately increase peel-associated phenolics and alkaloids while flesh softening accelerates, influencing handling and sensory outcomes. These findings align with I_{AD}-based maturity frameworks in other fruit systems, although calibration for pawpaw is needed[23–25]. There is also considerable promise for secondary metabolite research. Given the peel's intensive secondary metabolism and documented presence of acetogenins in pawpaw fruit tissues, peel valorization (e.g., functional ingredients) should proceed with targeted analytics and rigorous toxicological diligence[11,12].

The ethylene precursor availability remains steady across tissues and harvests; the regulatory network governing ripening becomes increasingly complex as pawpaw fruit matures. The coordinated rise in jasmonate-, ABA-, and auxin-linked metabolites after H2 highlights a shift toward hormonally integrated control of ethylene signaling that aligns with the onset of climacteric ripening (Supplementary Table S1). Martinez et al.[27] reported a clear ethylene climacteric peak during cherimoya ripening, paralleling the ethylene-linked metabolic patterns observed in pawpaw and other *Annona* species.

The sugar distribution in pawpaw is both harvest-dependent and tissue-specific, with the flesh serving as the primary site of energy-rich sugars that decline during maturation, while the peel maintains more stable levels of protective carbohydrates (Supplementary Table S2). This coordinated shift highlights the dual role of sugars in supporting fruit development and ensuring stress tolerance, reflecting an adaptive balance between metabolic activity and protective function. The observed sugar patterns in pawpaw are consistent with findings in *Asimina triloba* and related Annonaceae species, where sucrose is the dominant sugar accumulating in the pulp during ripening, contributing to sweetness and energy storage[28].

The tissue-specific fatty acids and lipid composition observed in pawpaw reflect functional specialization between peel and flesh. The peel is enriched in hydroxy fatty acids and saturated long-chain fatty acids, which are typical components of cuticular structures and contribute to protective barrier functions[29,30]. The presence of oxylipins such as 13(S)-HOT and sphingoid bases further supports a role in stress response and structural integrity[31]. In contrast, the flesh contains a higher diversity of oxylipins, including TriHOMEs and HODEs (Supplementary Table S3), indicating elevated lipid oxidation and signaling activity[32]. Additionally, the accumulation of highly oxygenated fatty acids and sphingolipid intermediates in the flesh suggests enhanced metabolic processes associated with fruit development and cellular regulation[33,34]. When compared to other Annonaceae species, there is some overlap between *Asimina triloba* and *Annona muricata* L. *Annona muricata* L. is widely known for its wide array of ethnopharmacological compounds; its strong bioactivity is the result of acetogenins and alkaloids[13]. The primary form of alkaloids in *Annona muricata* L. is benzylquinolines derived from tyrosine and phenolic compounds[13]; we were able to detect Squamocin K in the acetogenins category and other fatty acids, hydroxy fatty acids, and oxylipins (Supplementary Table S3). Among the metabolites identified, squamocin K (acetogenin), 9-HODE and 13-HODE (oxylipins), and phytosphingosine/sphinganine (sphingolipids) are of particular pharmaceutical interest. Squamocin K belongs to the annonaceous acetogenins, a class of potent mitochondrial complex I inhibitors that have demonstrated anticancer, antiparasitic, and cytotoxic activities[35,36]. The oxylipins 9-HODE and 13-HODE, which are products of linoleic acid oxidation, function as bioactive lipid mediators involved in inflammation, oxidative stress, macrophage differentiation, and cancer-related signaling pathways[37]. Similarly, phytosphingosine and sphinganine are biologically active sphingolipid metabolites that regulate apoptosis, cell proliferation, angiogenesis, and cellular signaling, and are increasingly recognized as important targets in cancer biology and therapeutic development. Therefore, the presence of these metabolites highlights potential pharmaceutical relevance related to oxidative stress regulation, inflammation, and anticancer mechanisms.

Conclusions

The findings from this study demonstrate that harvest timing and tissue exert strong, measurable influences on the physicochemical and metabolic characteristics of *Asimina triloba* 'Shenandoah™' fruit. Advancing harvest maturity was consistently associated with reductions in flesh firmness, dry matter, I_{AD} values, and lightness color parameters, alongside an increase in *a** coloration, reflecting progressive ripening and softening. Sun exposure further modulated these traits, indicating microenvironmental effects on fruit development. The widely targeted metabolomic analysis of 2,266 metabolites reveals a profound and highly integrated divergence between

https://doi.org/10.48130/frures-0026-0034

peel and flesh tissues, reflecting distinct physiological roles that intensify during fruit maturation. While both tissues exhibit stable and reproducible metabolic profiles, the peel maintains a significantly higher degree of metabolic turnover, particularly in secondary metabolites such as flavonoids and alkaloids, to function as a protective chemical shield. Conversely, the flesh focuses on primary metabolism, nutrient sequestration via ABC transporters, and the accumulation of flavor precursors during the transition from early to late-stage maturity. The presence of 728 core differentially accumulated metabolites and specialized K-means subclasses confirms that these tissue-specific signatures are driven by coordinated regulatory mechanisms, ensuring a synchronized response to environmental defense in the peel vs. nutritional development in the flesh. The progressive enrichment of jasmonate- and ABA-linked metabolites after mid-harvest underscores their coordinated contribution to the hormonal transition that drives pawpaw fruit toward full ripening. Pawpaw fruit shows a clear shift from high-energy sugars in the flesh to more protective sugars in the peel, reflecting distinct roles during maturation. These lipid-derived metabolites in peel and flesh tissues exhibit potential pharmaceutical value due to their roles in oxidative stress regulation, inflammation, cell signaling, and anticancer activity. Collectively, these results underscore that harvest timing is a critical determinant of pawpaw fruit quality, influencing not only sensory-relevant traits but also the biochemical composition of both peel and flesh. The distinct metabolic signatures identified here provide a foundation for optimizing harvest strategies to balance consumer acceptability with nutritional and bioactive value. Moreover, the metabolite richness of the peel highlights its potential as an underutilized source of valuable phytochemicals, warranting further exploration in functional food and phytopharmaceutical applications.

Author contributions

The authors confirm their contributions to the paper as follows: study conception, design and ideas: Al Shoffe Y; data collection organization and analysis, literature search: Al Shoffe Y, Erich GJ; manuscript drafting/revision: Al Shoffe Y, Erich GJ, Fei Z. All authors reviewed the results and approved the final version of the manuscript.

Data availability

All data from this study are available from the corresponding author upon reasonable request.

Acknowledgments

This work was supported in part by the Toward Sustainability Foundation through the Horticulture Section of the School of Integrative Plant Science, College of Agriculture and Life Sciences, Cornell University. Additional support was provided by the National Institute of Food and Agriculture, U.S. Department of Agriculture, through Multistate Project 1001075 (NE-2336), Improving Quality and Reducing Losses in Specialty Fruit Crops through Storage Technologies. This work was also partially supported by Metware Biotechnology Inc., MA, USA.

Conflict of interest

The authors declare that they have no conflict of interest.

Supplementary information accompanies this paper online at: https://doi.org/10.48130/frures-0026-0034.

Dates

Received 1 April 2026; Revised 22 June 2026; Accepted 20 August 2026; Published online 10 September 2026

References

[1] Pomper KW, Layne DR. 2010. The North American pawpaw: botany and horticulture. *Horticultural Reviews* 31:349–382

[2] Erich G, Peck G, Pritts M. 2025. Pawpaw: an underutilized tree with potential. *Journal of the American Pomological Society* 78:50–62

[3] Al Shoffe Y, Erich GJ, Baker-Porazinski O, Sun H, Fei Z. 2025. Optimizing harvest of pawpaw, the forgotten North American fruit, nondestructively to extend postharvest longevity. *Fruit Quarterly* 33:23–27

[4] Layne DR. 1996. The pawpaw [Asimina triloba (L.) Dunal]: a new fruit crop for Kentucky and the United States. *HortScience* 31:777–784

[5] Brannan RG, Anderson EE, Powell RL, Coyle MC. 2021. A comparative analysis of pawpaw (*Asimina triloba*) quality and nutritional data. *Journal of Applied Botany and Food Quality* 94:124–131

[6] Duffrin MW, Pomper KW. 2006. Development of flavor descriptors for pawpaw fruit puree: a step toward the establishment of a native tree fruit industry. *Family & Consumer Sciences Research Journal* 35:118–130

[7] Nam JS, Jang HL, Rhee YH. 2018. Nutritional compositions in roots, twigs, leaves, fruit pulp, and seeds from pawpaw (*Asimina triloba* [L.] Dunal) grown in Korea. *Journal of Applied Botany and Food Quality* 91:47–55

[8] Adainoo B, Crowell B, Thomas AL, Lin CH, Cai Z, et al. 2022. Physical characterization of frozen fruits from eight cultivars of the North American pawpaw (*Asimina triloba*). *Frontiers in Nutrition* 9:936192

[9] Brannan R, O'Neal D, Jawad M. 2025. Characterization of carotenoids and color in temperate *Asimina triloba* and comparison to other tropical Annonaceae fruits. *Exploration of Foods and Foodomics* 3:101098

[10] Roark ML. 2023. *Decoding the flavor of Kentucky's native pawpaw fruit*. Master's thesis. Eastern Kentucky University, Kentucky, USA. 81 pp https://encompass.eku.edu/etd/786

[11] McLaughlin JL. 2008. Paw paw and cancer: annonaceous acetogenins from discovery to commercial products. *Journal of Natural Products* 71:1311–1321

[12] Pomper KW, Lowe JD, Crabtree SB, Keller W. 2009. Identification of annonaceous acetogenins in the ripe fruit of the North American pawpaw (*Asimina triloba*). *Journal of Agricultural and Food Chemistry* 57:8339–8343

[13] Naik AV, Sellappan K. 2024. Quantification and histochemical localization of secondary metabolites during development in *Annona muricata* L. (Annonaceae). *Scientific Reports* 14:27641

[14] Al Shoffe Y, Nock JF, Zhang Y, Watkins CB. 2021. Physiological disorder development of 'Honeycrisp'apples after pre-and post-harvest 1-methycyclopropene (1-MCP) treatments. *Postharvest Biology and Technology* 182:111703

[15] Chen W, Gong L, Guo Z, Wang W, Zhang H, et al. 2013. A novel integrated method for large-scale detection, identification, and quantification of widely targeted metabolites: application in the study of rice metabolomics. *Molecular Plant* 6:1769–1780

[16] Fraga CG, Clowers BH, Moore RJ, Zink EM. 2010. Signature-discovery approach for sample matching of a nerve-agent precursor using liquid chromatography–mass spectrometry, XCMS, and chemometrics. *Analytical Chemistry* 82:4165–4173

[17] Kanehisa M, Goto S. 2000. KEGG: Kyoto encyclopedia of genes and genomes. *Nucleic Acids Research* 28:27–30

[18] Chong J, Xia J. 2018. MetaboAnalystR: an R package for flexible and reproducible analysis of metabolomics data. *Bioinformatics* 34:4313–4314

[19] Sawicka M, Latocha P, Łata B. 2023. Peel to flesh bioactive compounds ratio affect apple antioxidant potential and cultivar functional properties. *Agriculture* 13:478

[20] Zhang J, Gao N, Shu C, Cheng S, Sun X, et al. 2021. Phenolics profile and antioxidant activity analysis of kiwi berry (*Actinidia arguta*) flesh and peel extracts from four regions in China. *Frontiers in Plant Science* 12:689038

[21] Rather JA, Akhter N, Ayaz Q, Mir SA, Singh A, et al. 2023. Fruit peel valorization, phytochemical profile, biological activity, and applications in food and packaging industries: comprehensive review. *Current Food Science and Technology Reports* 1:63–79

[22] Sica VP, El-Elimat T, Oberlies NH. 2016. *In situ* analysis of *Asimina triloba* (paw paw) plant tissues for acetogenins via the droplet-liquid microjunction-surface sampling probe coupled to UHPLC-PDA-HRMS/MS. *Analytical Methods* 8:6143–6149

[23] Sadar N, Zanella A. 2019. A study on the potential of IAD as a surrogate index of quality and storability in cv. 'Gala'apple fruit. *Agronomy* 9:642

[24] Cocetta G, Beghi R, Mignani I, Spinardi A. 2017. Nondestructive apple ripening stage determination using the delta absorbance meter at harvest and after storage. *HortTechnology* 27:54–64

[25] Mostofi Y, DeEll JR. 2024. Variability of index of absorbance difference (I_{AD}) to indicate fruit maturity at harvest for major apple cultivars in Ontario. *Canadian Journal of Plant Science* 104:56–68

[26] Wood R, Peterson S. 1999. Lipids of the pawpaw fruit: *Asimina triloba*. *Lipids* 34:1099–1106

[27] Martinez G, Serrano M, Pretel MT, Amoros A, Riquelme F, et al. 1993. Ethylene biosynthesis during the ripening of cherimoya (*Annona cherimola*, Mill). In *Cellular and Molecular Aspects of the Plant Hormone Ethylene*, eds. Pech JC, Latché A, Balagué C. Dordrecht: Springer Netherlands. pp. 148–149 doi: 10.1007/978-94-017-1003-9_31

[28] Park SY, Jang HL, Nam JS. 2022. Comparison of nutritional compositions and physicochemical properties of unripe and ripe pawpaw (*Asimina triloba* [L.] Dunal) fruits grown in Korea. *Journal of the Korean Society of Food Science and Nutrition* 51:933–941

[29] Kolattukudy PE. 2001. Polyesters in higher plants. In *Biopolyesters*, eds. Babel W, Steinbüchel A. Berlin, Heidelberg: Springer. pp. 1–49 doi: 10.1007/3-540-40021-4_1

[30] Nawrath C. 2006. Unraveling the complex network of cuticular structure and function. *Current Opinion in Plant Biology* 9:281–287

[31] Wasternack C, Feussner I. 2018. The oxylipin pathways: biochemistry and function. *Annual Review of Plant Biology* 69:363–386

[32] Porta H, Rocha-Sosa M. 2002. Plant lipoxygenases. Physiological and molecular features. *Plant Physiology* 130:15–21

[33] Hannun YA, Obeid LM. 2018. Sphingolipids and their metabolism in physiology and disease. *Nature Reviews Molecular Cell Biology* 19:175–191

[34] Pata MO, Hannun YA, Ng CKY. 2010. Plant sphingolipids: decoding the enigma of the Sphinx. *New Phytologist* 185:611–630

[35] Duval RA, Duret P, Lewin G, Peris E, Hocquemiller R. 2005. Semisynthesis and biological activity of aminoacyl triesters of squamocin, an annonaceous acetogenin. *Bioorganic & Medicinal Chemistry* 13:3773–3781

[36] Shi JF, Wu P, Cheng XL, Wei XY, Jiang ZH. 2020. Synthesis and cytotoxic property of annonaceous acetogenin glycoconjugates. *Drug Design, Development and Therapy* 14:4993–5004

[37] Vangaveti V, Baune BT, Kennedy RL. 2010. Hydroxyoctadecadienoic acids: novel regulators of macrophage differentiation and atherogenesis. *Therapeutic Advances in Endocrinology and Metabolism* 1:51–60

Copyright: © 2026 by the author(s). Published by Maximum Academic Press, Fayetteville, GA. This article is an open access article distributed under Creative Commons Attribution License (CC BY 4.0), visit https://creativecommons.org/licenses/by/4.0/.